

Selective Si-C(sp³) Bond Cleavage Silyl-Bridged Amido Alkyl Ligand in an Yttrium Complex**

Jiamin Cai,^[a] Jie Zhang,^{*[a]} and Xigeng Zhou^{*[a]}

[a] Department of Chemistry, Shanghai Key Laboratory of Molecular Catalysis and Innovative Materials, Jiangwan Campus, Fudan University, Shanghai 200438, China.

* E-mail: zhangjie@fudan.edu.cn; xgzhou@fudan.edu.cn

Table of Contents

Table of Contents.....	1
1. X-ray Crystallographic Analysis of All New Complexes	2
2. Molecular structures of complex 6 ^H 、6 ^F and 6 ^{MeO}	5
3. NMR Spectra of All New Compounds	7
4. The spectra of in situ ¹ H NMR tracking experiments	15

1. X-ray Crystallographic Analysis of All New Complexes

Table S1. Crystal data and structure refinement for complexes **2**, **3** and **4**.

	2	3	4
Empirical formula	C ₃₉ H ₆₁ BN ₇ O ₂ Si ₃ Y	C ₂₄ H ₄₆ BN ₇ OSSi ₂ Y	C ₃₈ H ₅₈ BN ₈ OSi ₃ Y
Formula weight	844.93	635.63	826.91
Temperature/K	173.01	173.01	173
Crystal system	monoclinic	monoclinic	triclinic
Space group	P2 ₁ /c	P21/n	P-1
a/Å	17.3751(11)	11.0031(3)	9.7167(6)
b/Å	15.4894(10)	22.2150(8)	10.5316(7)
c/Å	16.8249(10)	14.0346(7)	22.2080(13)
α/°	90	90	87.551(2)
β/°	93.992(3)	108.192(2)	82.318(2)
γ/°	90	90	84.784(2)
Volume/Å ³	4517.1(5)	3259.1(2)	2241.8(2)
Z	4	4	2
ρ _{calc} (g/cm ³)	1.241	1.295	1.225
μ/mm ⁻¹	1.916	2.69	1.917
F(000)	1784	1336	872
Crystal size/mm ³	0.86 × 0.13 × 0.02	0.13 × 0.09 × 0.05	0.29 × 0.15 × 0.05
Radiation	GaKα (λ = 1.34138)	GaKα (λ = 1.34138)	GaKα (λ = 1.34138)
2θ range for data collection/°	6.658 to 114.144	6.726 to 137.468	6.992 to 105.99
Index ranges	-21 ≤ h ≤ 21, -19 ≤ k ≤ 19, -20 ≤ l ≤ 21	-15 ≤ h ≤ 15, -30 ≤ k ≤ 30, -19 ≤ l ≤ 18	-11 ≤ h ≤ 11, -12 ≤ k ≤ 12, -26 ≤ l ≤ 26
Reflections collected	67326	60567	67949
Independent reflections	9246 [R _{int} = 0.0707, R _{sigma} = 0.0419]	9130 [R _{int} = 0.5056, R _{sigma} = 0.1461]	7944 [R _{int} = 0.0509, R _{sigma} = 0.0275]
Data/restraints/parameters	9246/21/497	9130/0/346	7944/0/507
Goodness-of-fit on F ²	1.103	1.064	1.229
Final R indexes [I>=2σ(I)]	R ₁ = 0.0355, wR ₂ = 0.0886	R ₁ = 0.0854, wR ₂ = 0.1976	R ₁ = 0.0386, wR ₂ = 0.1118
Final R indexes [all data]	R ₁ = 0.0431, wR ₂ = 0.0979	R ₁ = 0.0955, wR ₂ = 0.2134	R ₁ = 0.0422, wR ₂ = 0.1253
Largest diff. peak and hole / e. Å ³	0.76/-0.43	1.73/-2.71	0.67/-0.76

Table S1. Crystal data and structure refinement for complexes **5**, **6^H** and **6^{MeO}**.

	5	6^H	6^{MeO}
Empirical formula	C ₄₈ H ₆₀ BN ₁₀ Si ₃ Y	C ₃₉ H ₆₀ BN ₈ OSi ₃ Y	C ₄₀ H ₆₂ BN ₈ O ₂ Si ₃ Y
Formula weight	961.05	840.94	870.96
Temperature/K	172.99	172.99	173
Crystal system	triclinic	triclinic	triclinic
Space group	P-1	P-1	P-1
a/Å	10.2029(4)	9.8288(6)	9.7543(3)
b/Å	10.7900(4)	10.6314(6)	10.6068(3)
c/Å	23.0484(7)	21.1115(12)	22.0190(7)
α/°	91.3010(10)	100.208(2)	98.8250(10)
β/°	97.5760(10)	90.122(2)	92.4230(10)
γ/°	95.7210(10)	95.118(2)	96.4810(10)
Volume/Å ³	2501.05(16)	2162.1(2)	2232.65(12)
Z	2	2	2
ρ _{calc} (g/cm ³)	1.276	1.292	1.296
μ/mm ⁻¹	1.766	1.993	1.953
F(000)	1008	888	920
Crystal size/mm ³	0.08 × 0.07 × 0.04	0.18 × 0.07 × 0.06	0.22 × 0.12 × 0.07
Radiation	GaKα (λ = 1.34138)	GaKα (λ = 1.34138)	GaKα (λ = 1.34138)
2θ range for data collection/°	7.168 to 89.882	7.382 to 112.734	7.672 to 102.748
Index ranges	-10 ≤ h ≤ 10, -11 ≤ k ≤ 11, -24 ≤ l ≤ 24	-12 ≤ h ≤ 12, -13 ≤ k ≤ 13, -26 ≤ l ≤ 25	-11 ≤ h ≤ 11, -12 ≤ k ≤ 12, -25 ≤ l ≤ 25
Reflections collected	20829	30186	27407
Independent reflections	6118 [R _{int} = 0.0702, R _{sigma} = 0.0691]	8489 [R _{int} = 0.0593, R _{sigma} = 0.0540]	7355 [R _{int} = 0.0692, R _{sigma} = 0.0613]
Data/restraints/parameters	6118/0/586	8489/0/496	7355/0/514
Goodness-of-fit on F ²	1.022	1.087	1.08
Final R indexes [I >= 2σ (I)]	R ₁ = 0.0407, wR ₂ = 0.0824	R ₁ = 0.0570, wR ₂ = 0.1785	R ₁ = 0.0499, wR ₂ = 0.1362
Final R indexes [all data]	R ₁ = 0.0623, wR ₂ = 0.0913	R ₁ = 0.0632, wR ₂ = 0.1852	R ₁ = 0.0579, wR ₂ = 0.1429
Largest diff. peak and hole / e. Å ⁻³	0.35/-0.52	2.32/-1.38	1.29/-0.88

Table S3. Crystal data and structure refinement for complexes **6^f** and **7**.

6^f	
Empirical formula	C ₃₉ H ₅₉ BFN ₈ OSi ₃ Y
Formula weight	858.93
Temperature/K	173
Crystal system	triclinic
Space group	P-1
a/Å	9.7140(3)
b/Å	10.5154(3)
c/Å	21.8740(7)
α/°	98.5180(10)
β/°	93.9370(10)
γ/°	94.1280(10)
Volume/Å ³	2196.84(12)
Z	2
ρ _{calc} (g/cm ³)	1.298
μ/mm ⁻¹	1.991
F(000)	904
Crystal size/mm ³	0.22 × 0.14 × 0.12
Radiation	GaKα (λ = 1.34138)
2θ range for data collection/°	7.724 to 100.878
Index ranges	-11 ≤ h ≤ 11, -12 ≤ k ≤ 12, -25 ≤ l ≤ 25
Reflections collected	21343
Independent reflections	6956 [R _{int} = 0.0427, R _{sigma} = 0.0403]
Data/restraints/parameters	6956/0/499
Goodness-of-fit on F ²	1.039
Final R indexes [I>=2σ(I)]	R ₁ = 0.0379, wR ₂ = 0.1040
Final R indexes [all data]	R ₁ = 0.0393, wR ₂ = 0.1053
Largest diff. peak and hole / e. Å ³	1.65/-0.58

2. Molecular structures of complex $\mathbf{6^H}$, $\mathbf{6^F}$ and $\mathbf{6^{MeO}}$

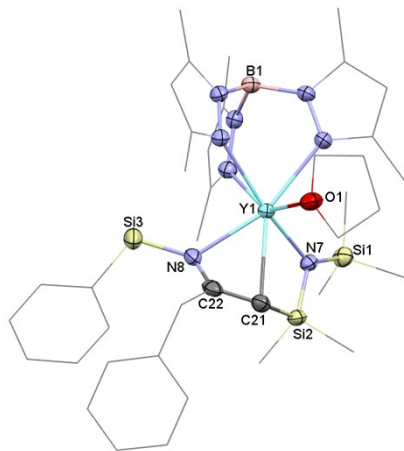


Figure S1 ($\mathbf{6^H}$)

Molecular structure of $\mathbf{6^H}$. Thermal ellipsoids are set at 50% probability level. H atoms are not shown for clarity. Selected bond lengths [\AA] and angles [°] : Y1-N8 2.340(3), Y1-N7 2.261(3), N8-C22 1.367(5), C21-C22 1.369(6), C22-C23 1.531(6), Si2-C21 1.872(4), Si2-N7 1.707(3), Si1-N7 1.713(3), Si3-N8 1.704(4); N8-Y1-N7 99.03(8), N8-C22-C21 119.9(3), C22-C21-Si2 128.4(3), C21-Si2-N7 107.77(16), Y1-N7-Si2 99.24(14).

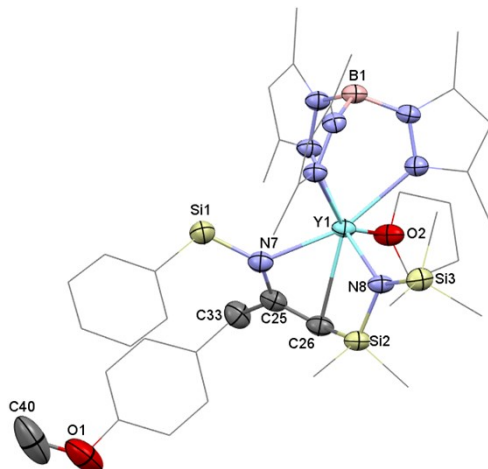


Figure S2 ($\mathbf{6^{MeO}}$)

Molecular structure of $\mathbf{6^{MeO}}$. Thermal ellipsoids are set at 50% probability level. H atoms are not shown for clarity. Selected bond lengths [\AA] and angles [°] : Y1-N7 2.326(3), N7-C25 1.362(4), C26-C25 1.373(5), Si2-C26 1.869(3), Si2-N8 1.707(3), Si1-N7 1.708(3), Si3-N8 1.708(3), C25-C33 1.536(5); N8-Y1-N7 98.80(10), C25-N7-Y1 92.9(2), C25-C26-Si2 129.1(3), N8-Si2-C26 108.26(14), Si2-N8-Y1 99.39(12).

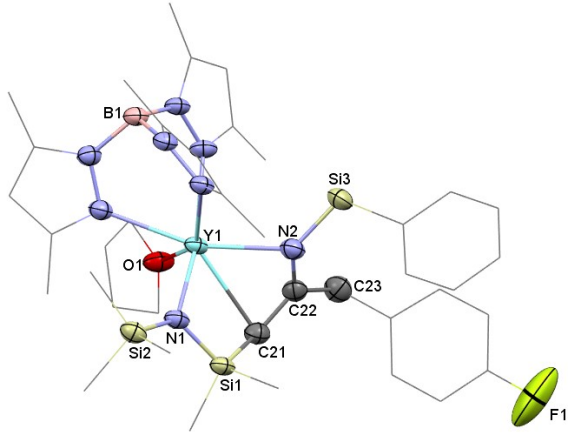


Figure S3 (6^f)

Molecular structure of **6^f**. Thermal ellipsoids are set at 50% probability level. H atoms are not shown for clarity. Selected bond lengths [Å] and angles [°] : Y1-N1 2.263(2), Y1-N2 2.331(2), N1-Si1 1.706(2), N1-Si2 1.711(2), C21-Si1 1.876(3), C21-C22 1.375(4), C22-C23 1.529(4), N2-C22 1.367(4), N2-Si3 1.705(2); N1-Y1-N2 99.02(8), N1-Si1-C21 108.18(12), C22-C21-Si1 128.9(2), C21-C22 C23 118.8(3), N2-C22-C21 120.5(3), N2-C22-C23 120.6(3), C22-N2-Y1 92.33(16).

3. NMR Spectra of All New Compounds

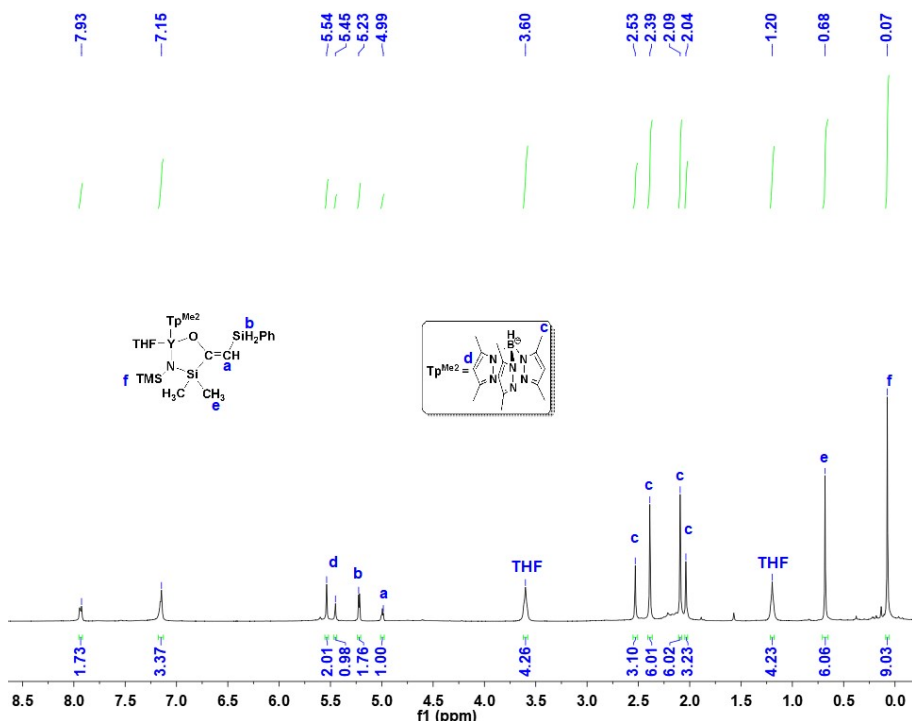


Figure S4. ^1H NMR spectrum of complex 2 in C_6D_6 at room temperature.

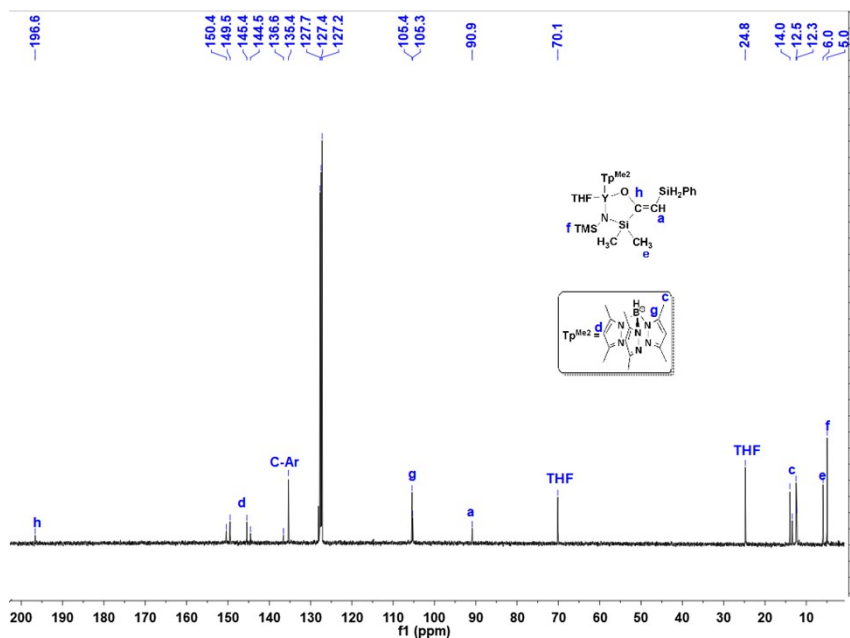


Figure S5. $^{13}\text{C}\{^1\text{H}\}$ NMR NMR spectrum of complex 2 in C_6D_6 at room temperature.

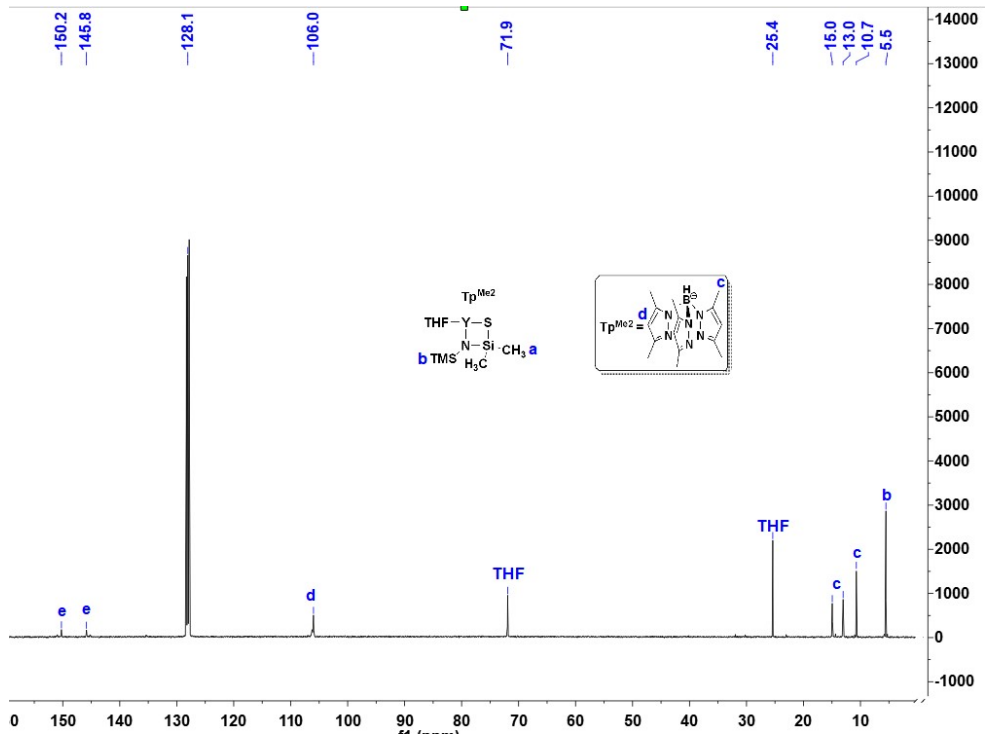
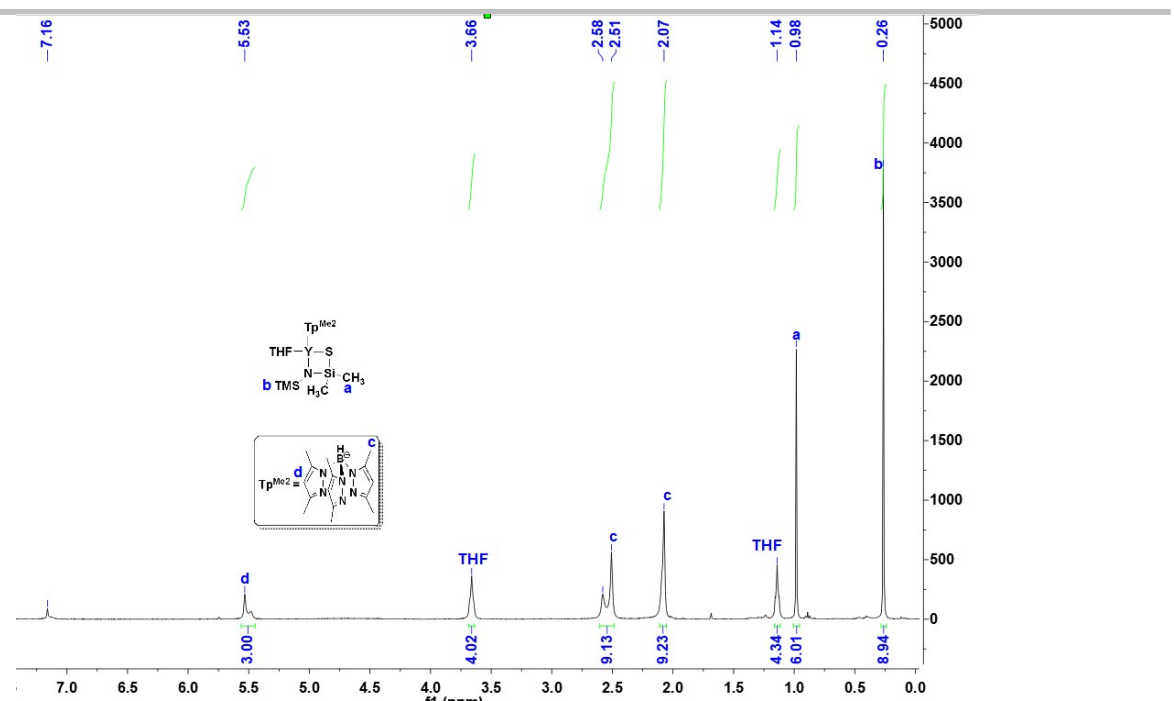


Figure S7. $^{13}\text{C}\{^1\text{H}\}$ NMR spectrum of complex **3** in C_6D_6 at room temperature.

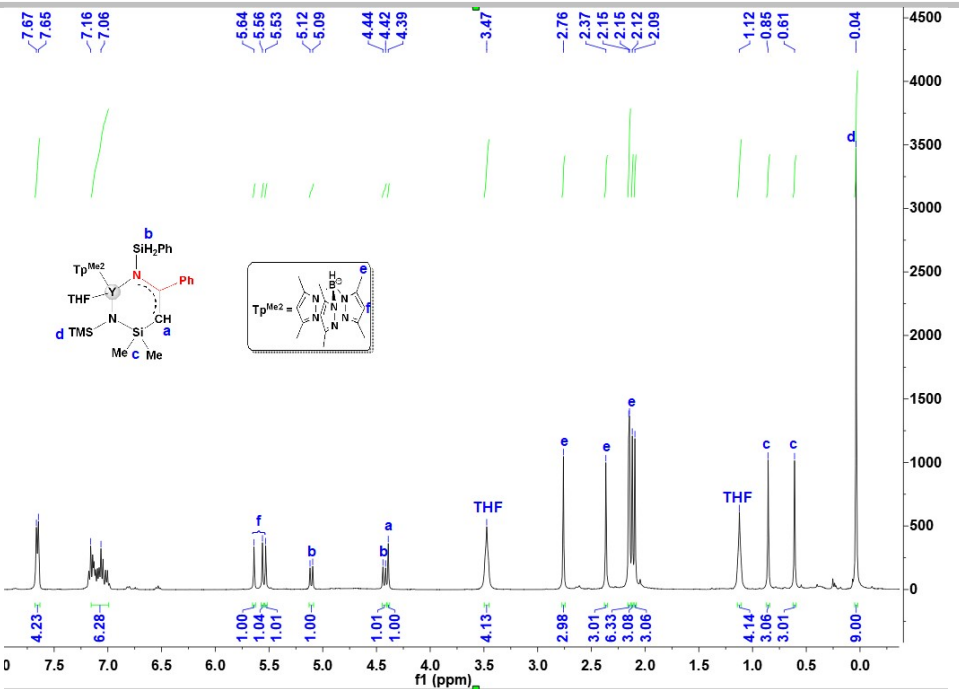


Figure S8. ^1H NMR spectrum of complex 4 in C_6D_6 at room temperature.

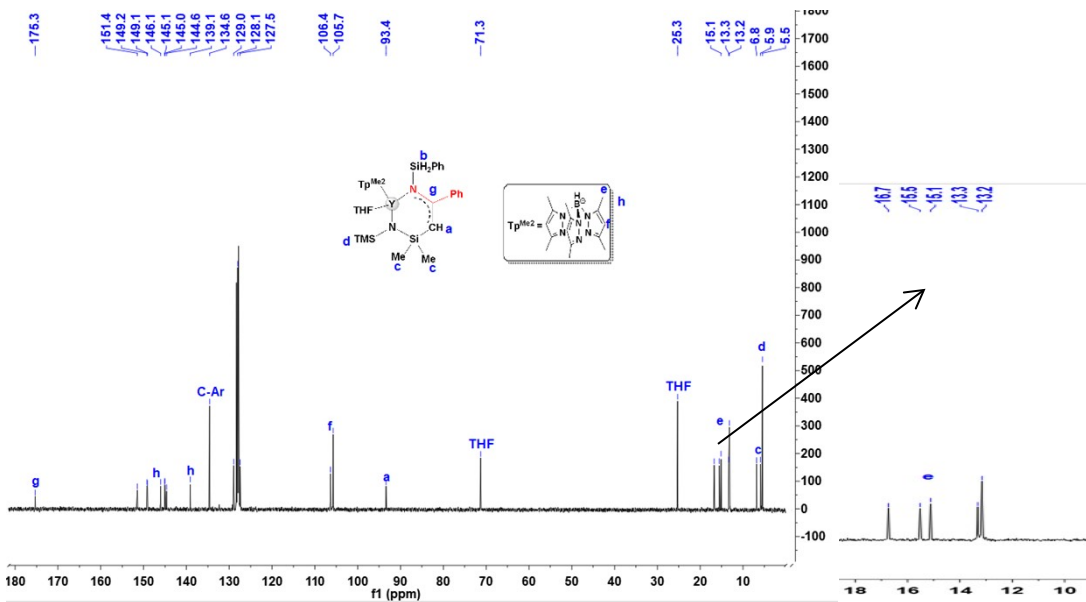


Figure S9. $^{13}\text{C}\{\text{H}\}$ NMR spectrum of complex **4** in C_6D_6 at room temperature.

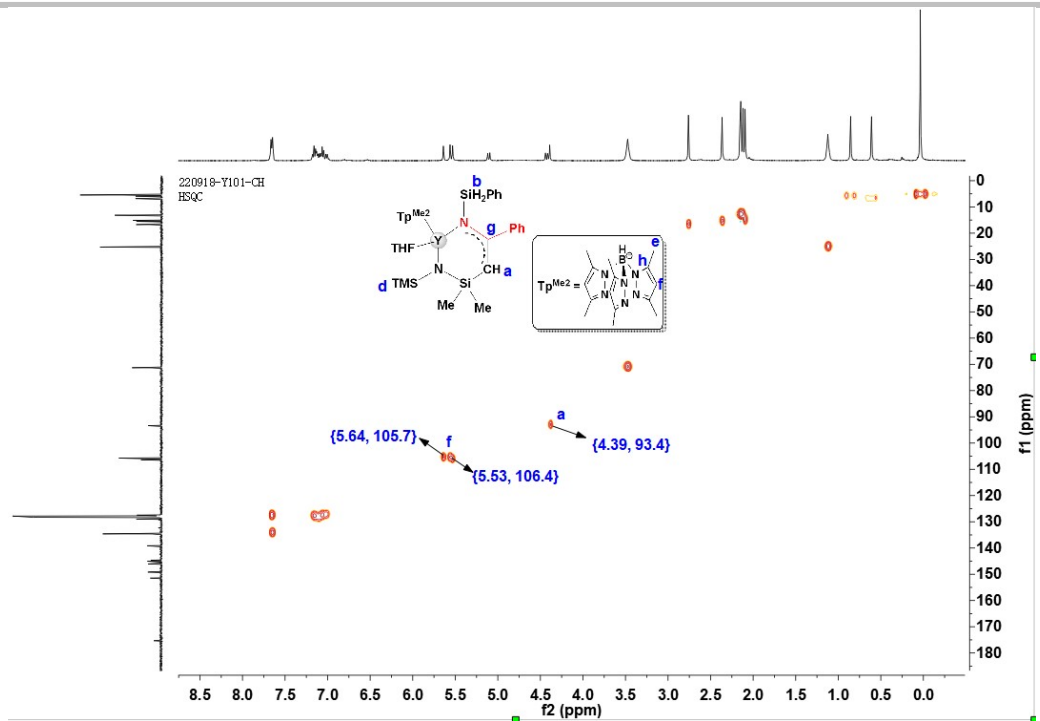


Figure S10. HSQC (^1H NMR - ^{13}C NMR) Spectrum of **4** in C_6D_6 at room temperature.

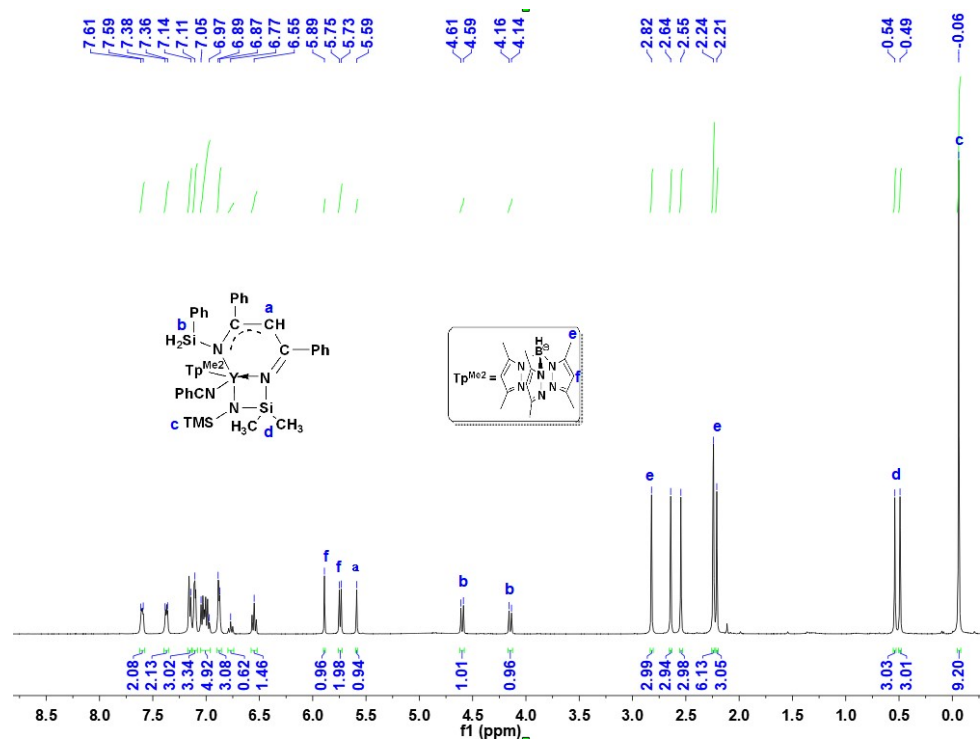


Figure S11. ^1H NMR spectrum of complex **5** in C_6D_6 at room temperature.

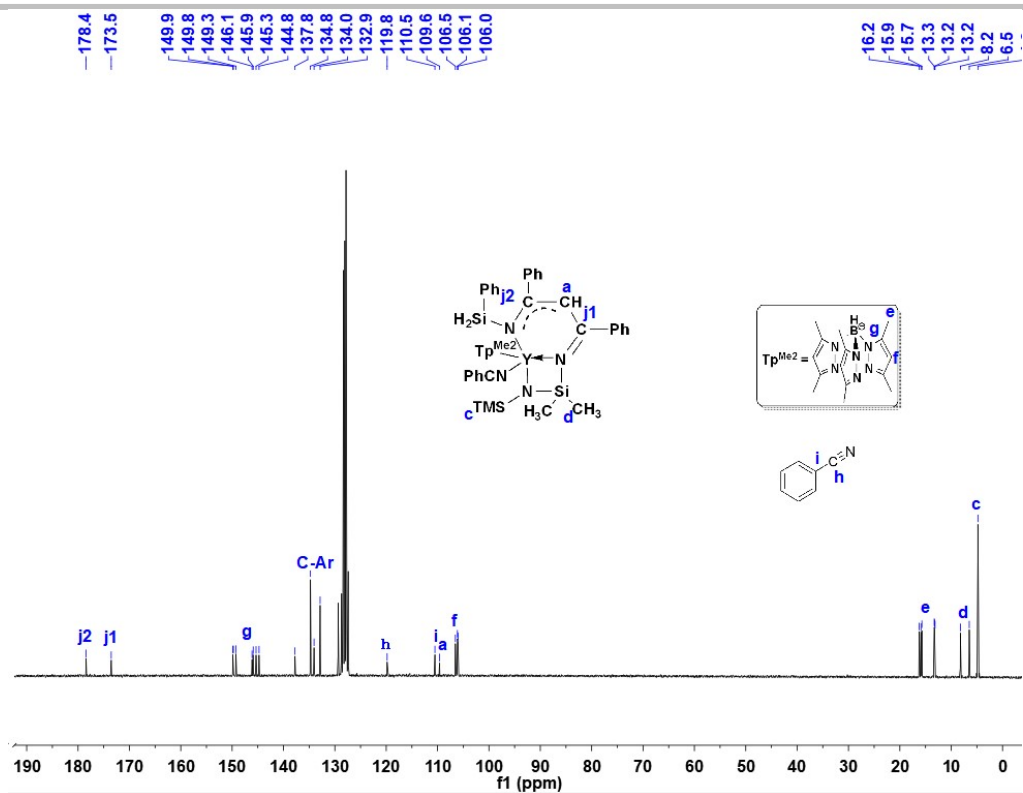


Figure S12. $^{13}\text{C}\{\text{H}\}$ NMR spectrum of complex **5** in C_6D_6 at room temperature.

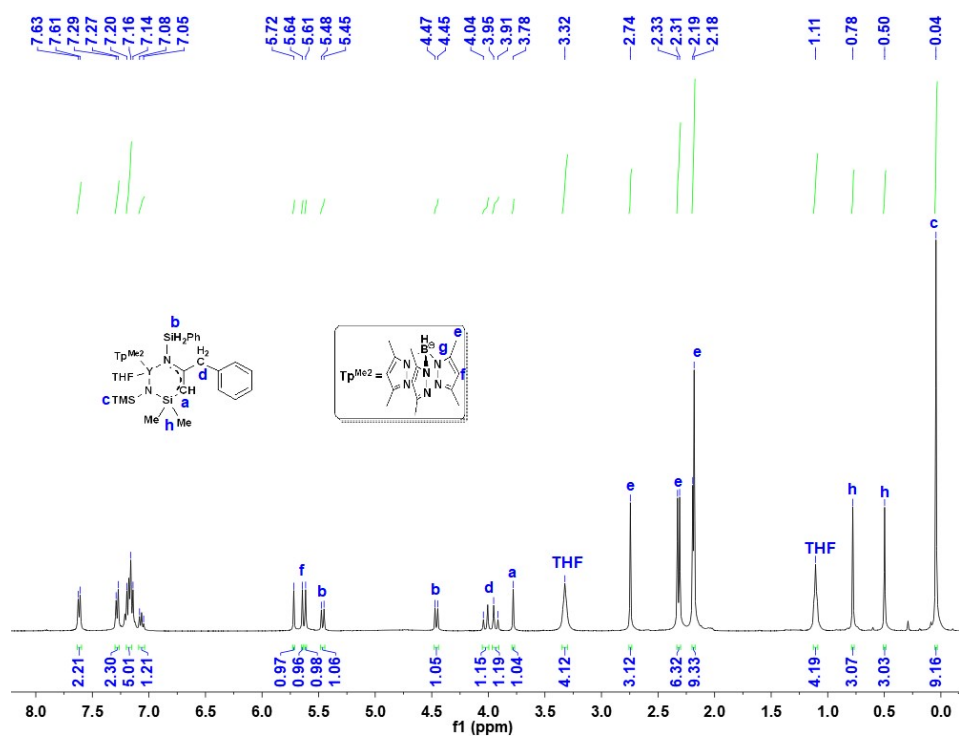


Figure S13. ^1H NMR spectrum of complex **6^H** in C_6D_6 at room temperature.

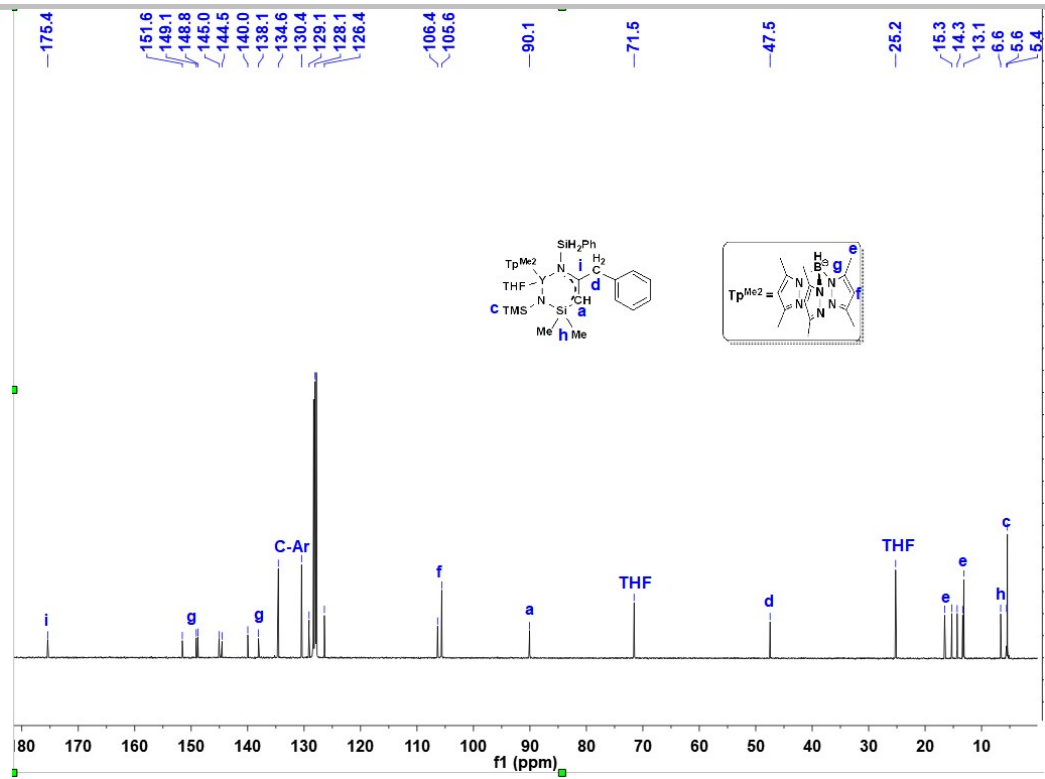


Figure S14. $^{13}\text{C}\{\text{H}\}$ NMR spectrum of complex **6^H** in C₆D₆ at room temperature.

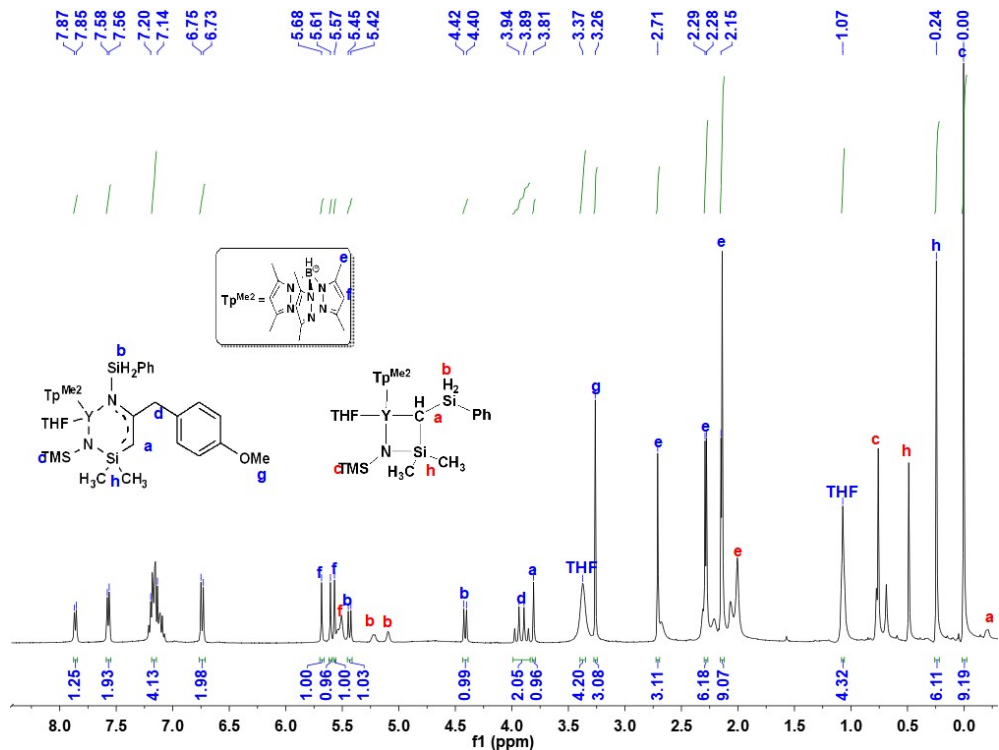


Figure S15. ^1H NMR spectrum of complex **6^{MeO}** in C_6D_6 at room temperature.

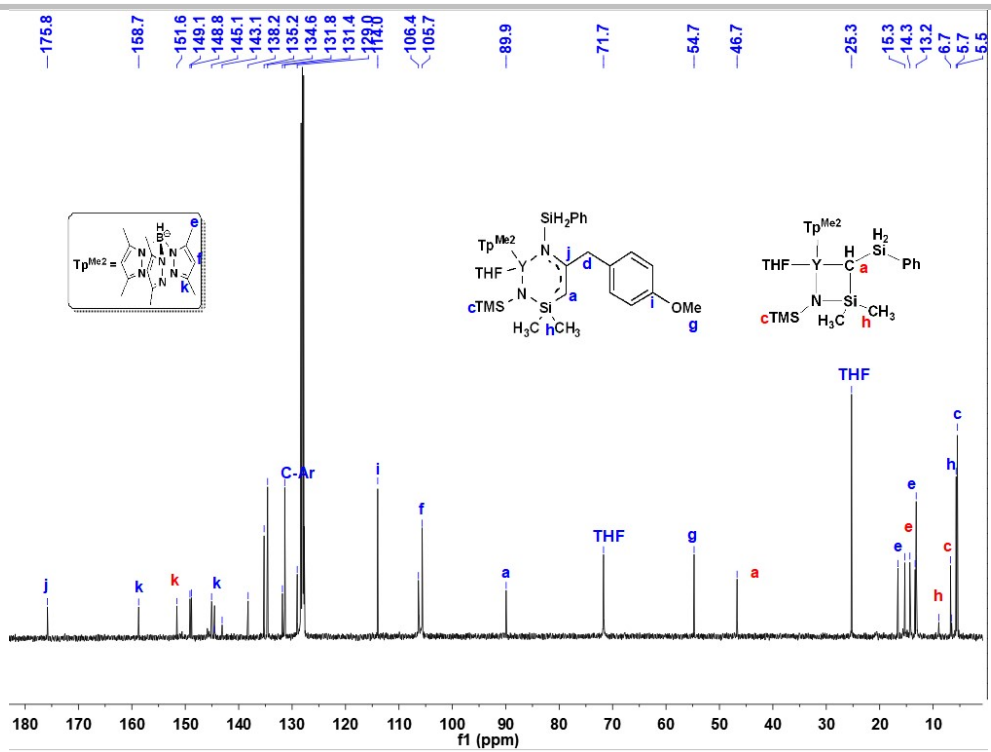


Figure S16. $^{13}\text{C}\{^1\text{H}\}$ NMR spectrum of complex $\mathbf{6}^{\text{MeO}}$ in C_6D_6 at room temperature.

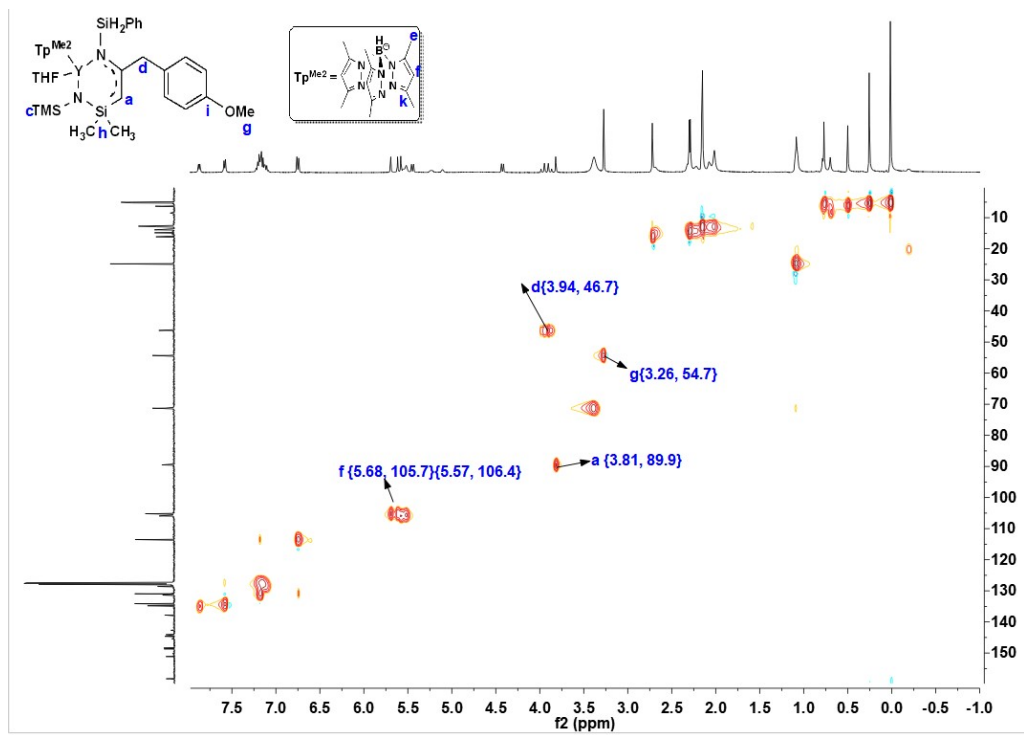


Figure S17. HSQC (^1H NMR - ^{13}C NMR) Spectrum of $\mathbf{6}^{\text{MeO}}$ in C_6D_6 at room temperature.

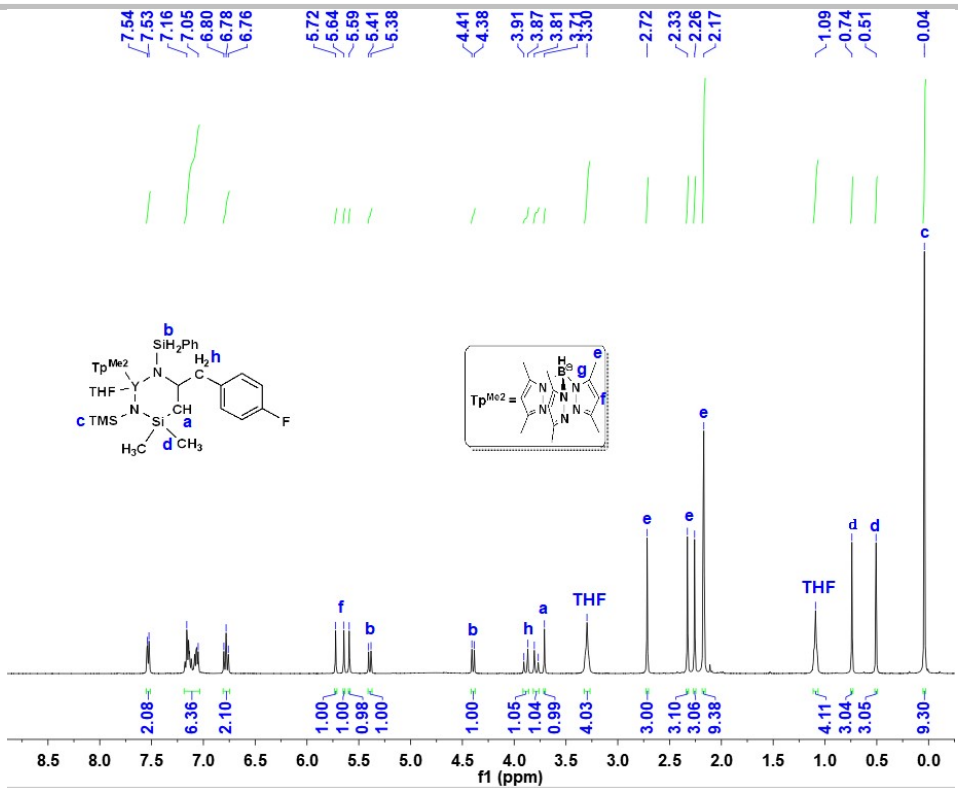


Figure S18. ^1H NMR spectrum of complex **6F** in C_6D_6 at room temperature.

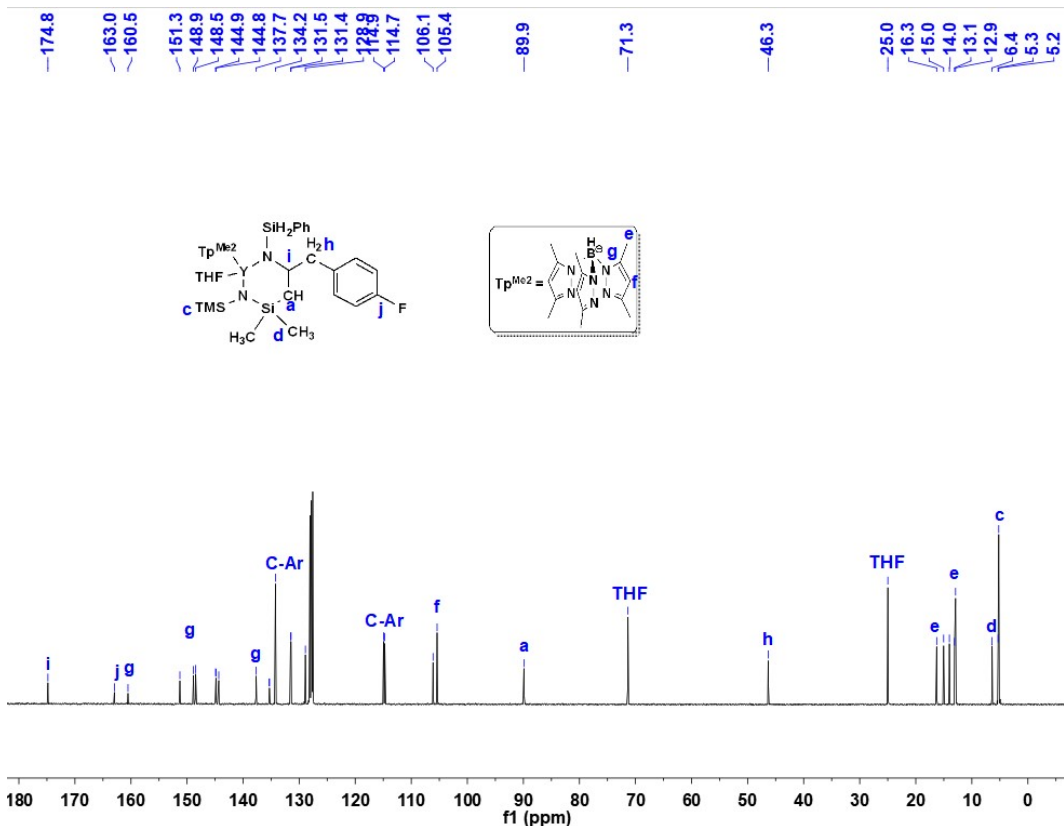


Figure S19. $^{13}\text{C}\{{}^1\text{H}\}$ NMR spectrum of complex **6F** in C_6D_6 at room temperature.

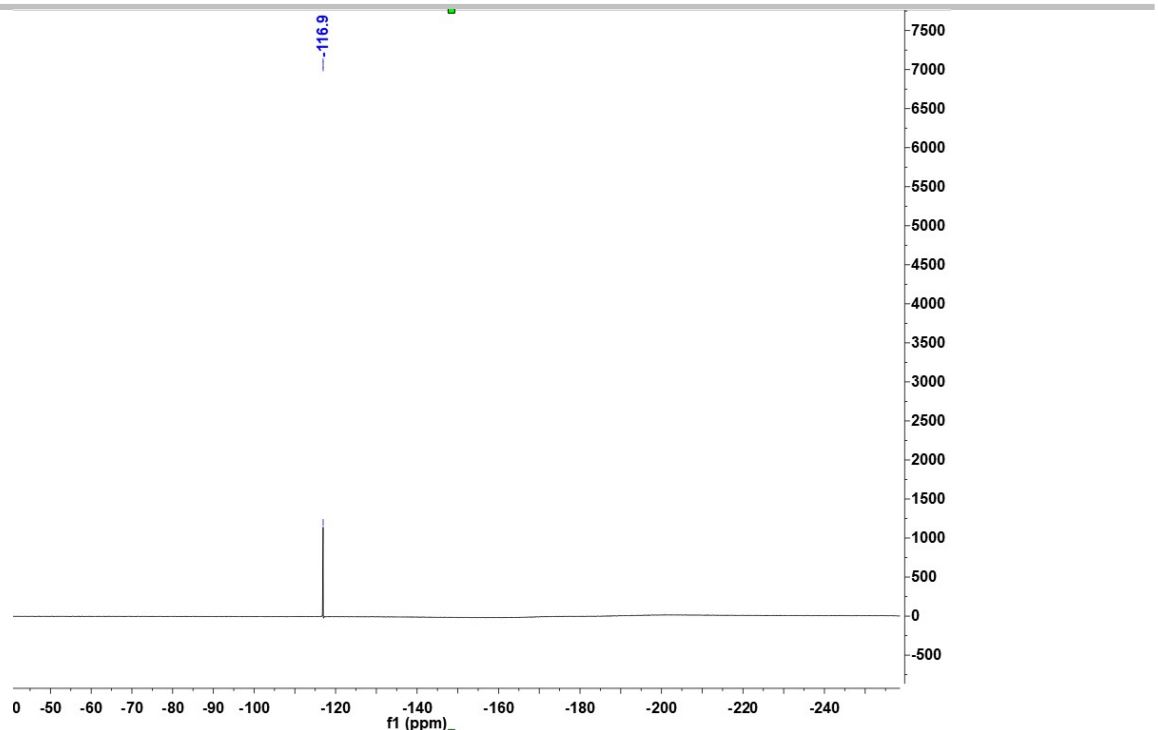


Figure S20. ^{19}F NMR spectrum of complex $\mathbf{6}^{\text{F}}$ in C_6D_6 at room temperature.

4. The spectra of in situ ^1H NMR tracking experiments

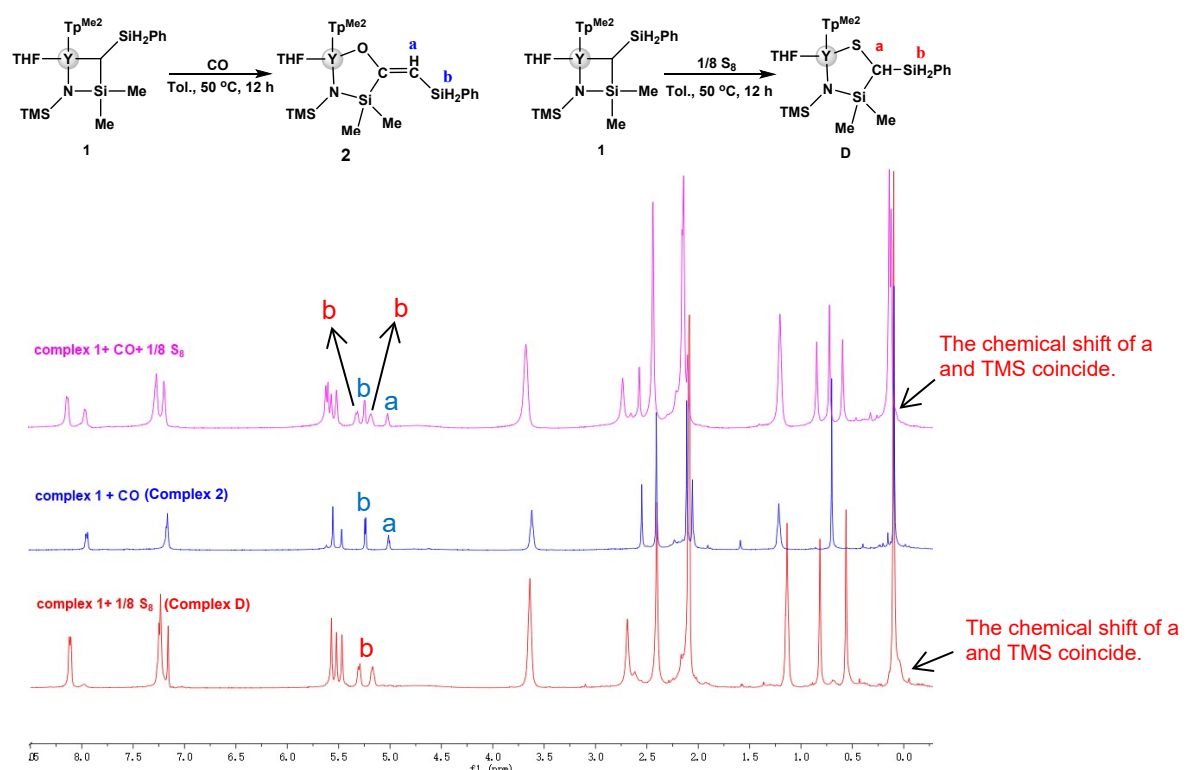


Figure S21. The in situ ^1H NMR spectra of the reaction of **1**, CO, and $1/8 \text{S}_8$ in C_6D_6 (Attempt to obtain the crystal structure was unsuccessful due to poor crystalline sample).

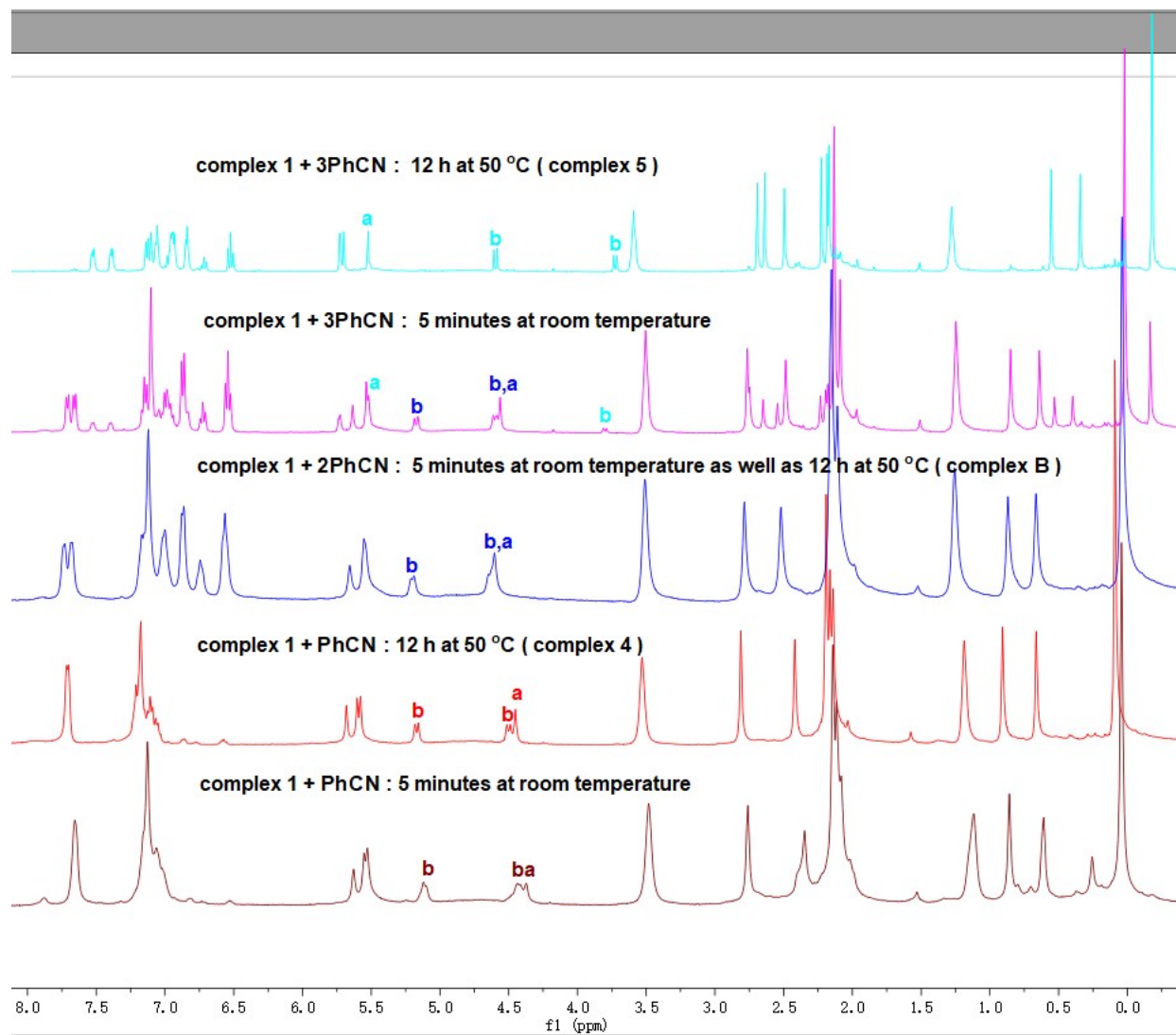
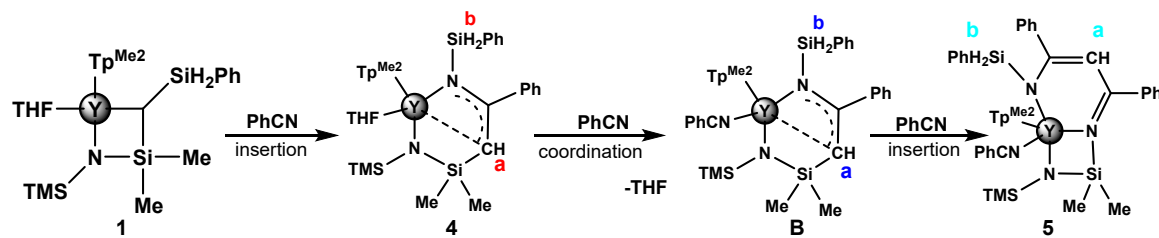


Figure S22. The *in situ* ^1H NMR spectra of stepwise reactions of **1** and PhCN with different molar ratio in C_6D_6 . (the *in situ* NMR experiments were done at room temperature or 50°C (see the title of each spectrum), but their NMR spectra were recorded at room temperature)

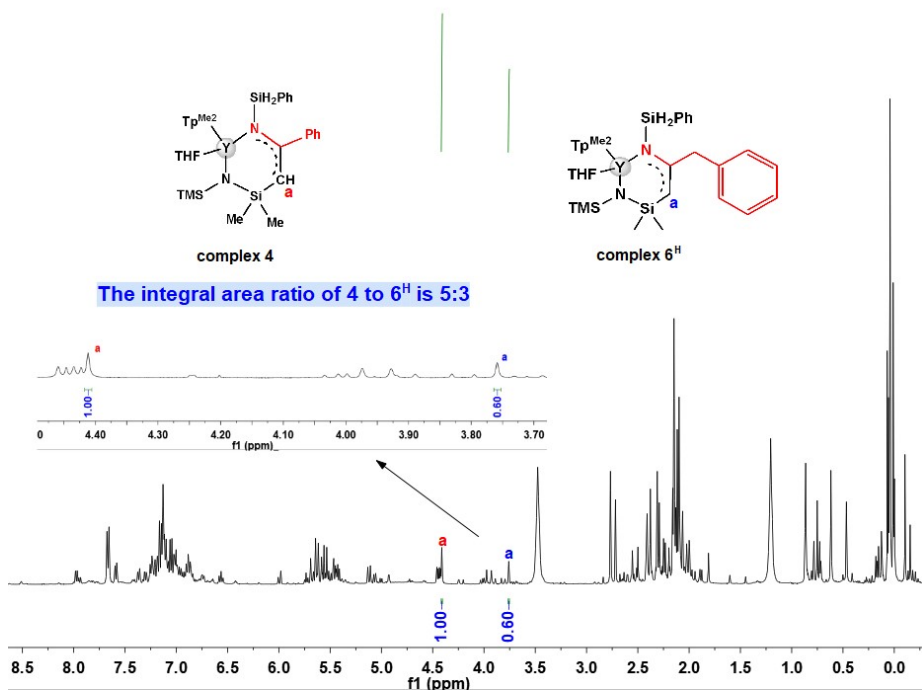


Figure S23. The in situ ^1H NMR spectra of competitive reactions of **1** with equimolar **PhCN** and **BnCN** in C_6D_6 .

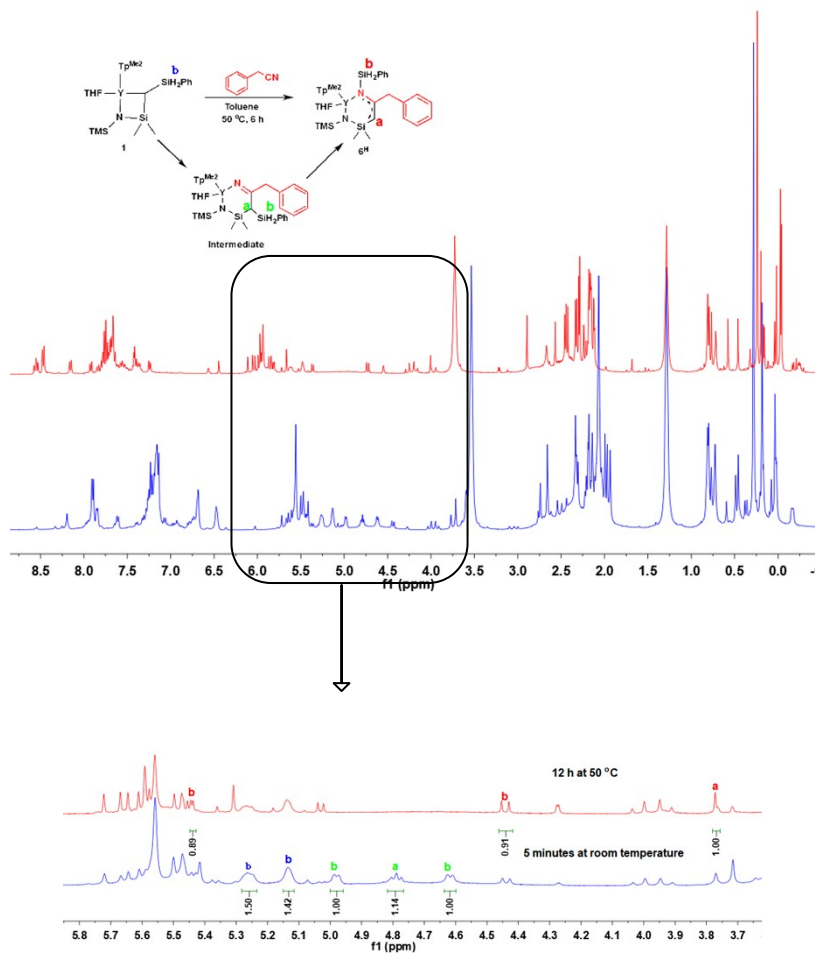


Figure S24. The in situ ^1H NMR spectra of reactions of **1** with equimolar $\text{C}_6\text{H}_4\text{CH}_2\text{CN}$ in C_6D_6 .

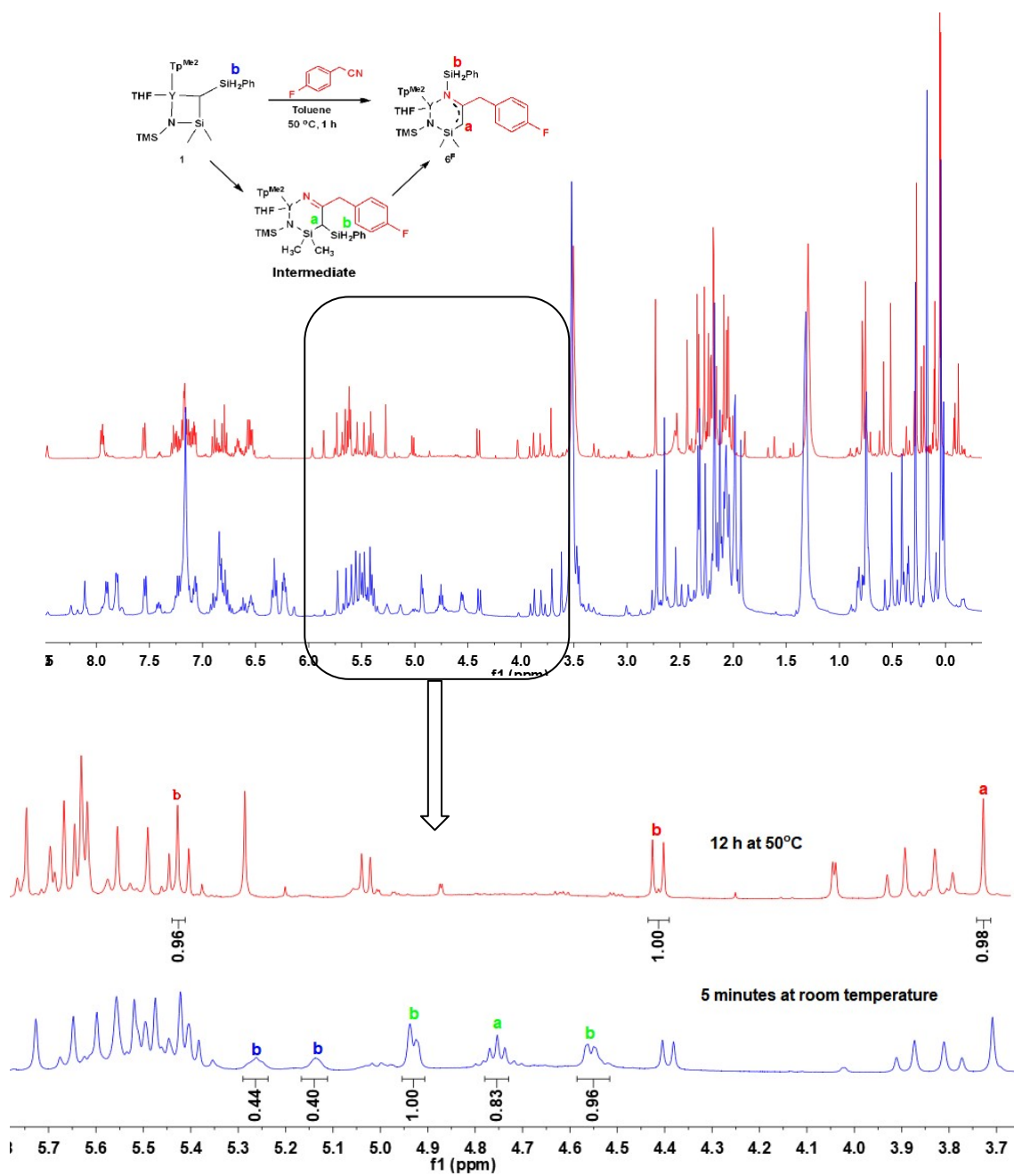


Figure S25. The *in situ* ^1H NMR spectra of reactions of **1** with equimolar $p\text{-MeO-C}_6\text{H}_4\text{CH}_2\text{CN}$ in C_6D_6 .

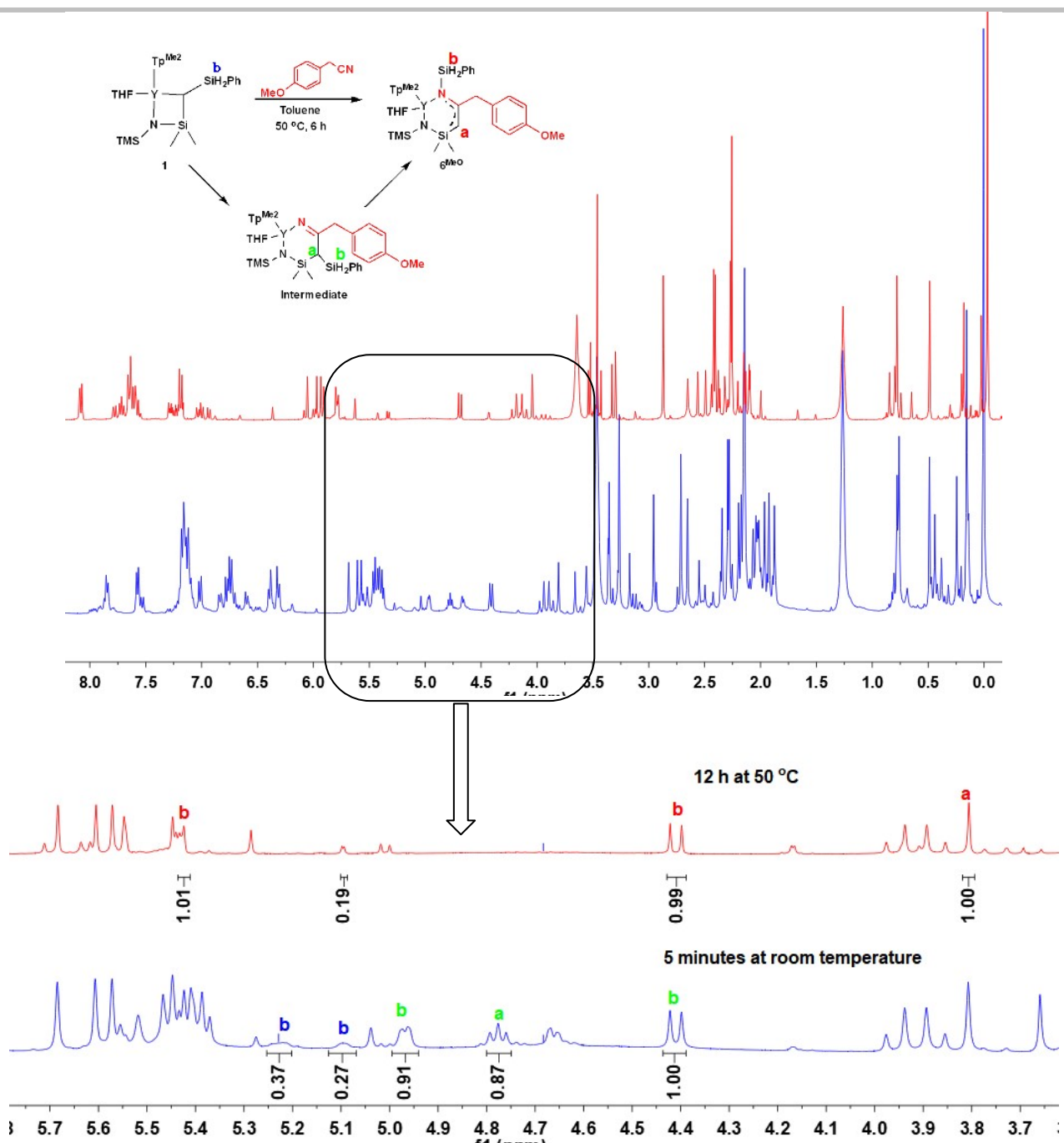


Figure S26. The *in situ* ^1H NMR spectra of reactions of **1** with equimolar $p\text{-F-C}_6\text{H}_4\text{CH}_2\text{CN}$ in C_6D_6 .